Scattering and Radiation from Finite Thick Slits in Parallel-Plate Waveguide

Jung H. Lee, Hyo Joon Eom, *Member, IEEE*, and Jae W. Lee

***Abstract*— The problem of TE-wave scattering and radiation from a finite number of thick slits in a parallel-plate waveguide is solved. The Fourier transform is used to express the scattered field in the spectral domain. The boundary conditions are enforced to obtain a series solution which is amenable to numerical computation. The numerical computations are performed to illustrate the behaviors of scattering, transmission, and reflection in terms of incident angle, slit size and operating frequency. The presented solution is computationally very efficient so that it is useful for slotted-waveguide leaky-wave antenna applications.**

I. INTRODUCTION

ELECTROMAGNETIC radiation and scattering from a thin-slotted parallel-plate waveguide has been extensively studied in [1]–[3] for leaky-wave antenna applications. The radiation from the thick slot was studied in [4] by assuming that thick metal strips were periodically loaded over a dielectric waveguide on a conducting plane. The motivation of the present paper is to investigate TE-wave scattering and radiation from a finite number of thick slits in a parallel-plate waveguide. Our assumption of a finite number of slits is not only realistic but also versatile in that it allows us to investigate cases ranging from a single to infinite thick slits. Using the Fourier transform and the residue calculus, in the next section we represent the transmission, reflection, and scattering coefficients in fast-convergent series form which is computationally very efficient. The notations in this paper closely follow those in [5].

II. FIELD REPRESENTATIONS

N slits of width $2a$ and depth d in a parallel-plate waveguide are shown in Fig. 1. Regions (I), (II), and (III), respectively, denote the parallel-plate waveguide (wavenumber $= k_1 = \omega\sqrt{\mu_1\epsilon_1}$), $N(= L_1 + L_2 + 1)$ slits (wavenumber $= k_2 = \omega\sqrt{\mu_2\epsilon_2}$), and the lower half-space (wavenumber $= k_3 = \omega\sqrt{\mu_3\epsilon_3} = 2\pi/\lambda$). We assume that two incident TE-waves, E_y^{i1} and E_y^{i2}, excite Regions (I) and (III), respectively. A time-harmonic factor $e^{-i\omega t}$ is suppressed. In Region (I), the total field consists of the incident and scattered fields

$$E_y^{i1}(x,z) = A_1 e^{ik_{xs}x}\sin k_{zs}(z+b) \tag{1}$$

$$E_y^{I}(x,z) = \frac{i}{\pi}\int_{-\infty}^{\infty}\tilde{E}_y^{I}(\zeta)\sin(\kappa_1 z)e^{-i\zeta x}\,d\zeta \tag{2}$$

Manuscript received July 13, 1994; revised June 22, 1995.

The authors are with the Department of Electrical Engineering, Korea Advanced Institute of Science and Technology, 373-1, Kusong Dong, Yusung Gu, Taejon, Korea.

Publisher Item Identifier S 0018-926X(96)01205-7.

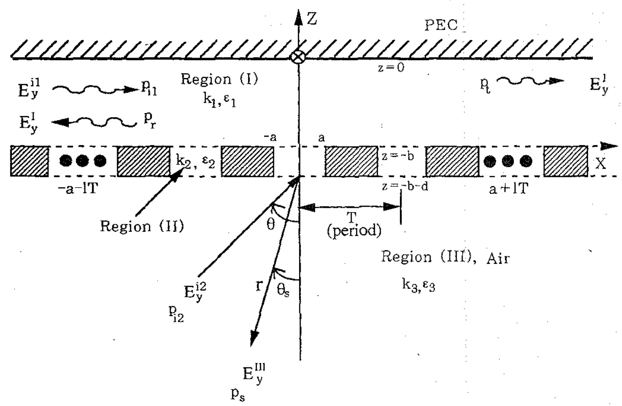

Fig. 1. Problem geometry of slotted waveguide leaky-wave antenna.

where $0 < s < k_1 b/\pi$ (s: *integer*), $k_{zs} = s\pi/b$, $k_{xs} = \sqrt{k_1^2 - k_{zs}^2}$, $\kappa_1 = \sqrt{k_1^2 - \zeta^2}$.

In Region (II), $(lT - a < x < lT + a, -d-b < z < -b$: $l = -L_1, \cdots, L_2)$ the total transmitted field is

$$E_y^{II}(x,z) = \sum_{m=1}^{\infty}\sin a_m(x+a-lT)[b_m^l\cos\xi_m(z+b) + c_m^l\sin\xi_m(z+b)] \tag{3}$$

where $a_m = m\pi/(2a)$ and $\xi_m = \sqrt{k_2^2 - a_m^2}$.

In Region (III) the total field is

$$E_y^{i2}(x,z) = A_2 e^{i[k_x x + k_z(z+b+d)]} \tag{4}$$

$$E_y^{r}(x,z) = -A_2 e^{i[k_x x - k_z(z+b+d)]} \tag{5}$$

$$E_y^{III}(x,z) = \frac{1}{2\pi}\int_{-\infty}^{\infty}\tilde{E}_y^{III}(\zeta)e^{-i\zeta x - i\kappa_3(z+b+d)}\,d\zeta \tag{6}$$

where $\kappa_3 = \sqrt{k_3^2 - \zeta^2}$, $k_x = k_3\sin\theta$, and $k_z = k_3\cos\theta$.

The tangential electric field continuity at $z = -b$ yields

$$E_y^{I}(x,-b) = \begin{cases} E_y^{II}(x,-b), & lT - a < x < lT + a \\ 0, & \text{otherwise.}\end{cases} \tag{7}$$

Applying the Fourier transform $\int_{-\infty}^{\infty}(\cdots)e^{i\zeta x}\,dx$ to (7) yields

$$\tilde{E}_y^{I}(\zeta)[-2i\sin(\kappa_1 b)] = \sum_{l=-L_1}^{L_2}\sum_{m=1}^{\infty} b_m^l a_m e^{i\zeta lT}a^2 F_m(a\zeta) \tag{8}$$

$$F_m(t) = \frac{e^{it}(-1)^m - e^{-it}}{t^2 - (m\pi/2)^2}. \tag{9}$$

The tangential magnetic field continuity on the aperture of the slits $(rT - a < x < rT + a, z = -b: r = -L_1, \cdots, L_2)$ gives

$$\frac{ik_{zs}}{\mu_1} A_1 e^{ik_{xs}x} - \frac{1}{\pi\mu_1}\int_{-\infty}^{\infty} \kappa_1 \tilde{E}_y^{\mathrm{I}}(\zeta)\cos(\kappa_1 b)e^{-i\zeta x}\, d\zeta = \frac{i}{\mu_2}\sum_{m=1}^{\infty} c_m^l \xi_m \sin a_m(x + a - lT). \quad (10)$$

Substituting $\tilde{E}_y^{\mathrm{I}}(\zeta)$ of (8) into (10), multiplying $\int_{rT-a}^{rT+a}(\cdots)\sin a_n(x + a - rT)\; dx$, and performing integration, we obtain

$$\frac{k_{zs}A_1}{\mu_1}\gamma_n^r - \frac{1}{2\pi\mu_1}\sum_{l=-L_1}^{L_2}\sum_{m=1}^{\infty} b_m^l a_m a_n a^2 I_{1mn}^{rl} = \frac{1}{\mu_2}c_n^r \xi_n a \quad (11)$$

where

$$\gamma_n^r = a_n e^{ik_{xs}rT}a^2 F_n(k_{xs}a) \quad (12)$$

$$I_{1mn}^{rl} = \int_{-\infty}^{\infty} \kappa_1 \cot(\kappa_1 b)a^2 F_m(\zeta a)F_n(-\zeta a)e^{i\zeta(l-r)T}\, d\zeta. \quad (13)$$

The evaluation of I_{1mn}^{rl} using the residue calculus gives [5]

$$I_{1mn}^{rl} = \frac{2\pi\eta_m \cot(\eta_m b)}{aa_m^2}\delta_{nm}\delta_{rl} + J_{1mn}^{rl} \quad (14)$$

(15), shown at the bottom of the page, where δ_{nm} is the Kronecker delta, $\eta_m = \sqrt{k_1^2 - a_m^2}$, and J_{1mn}^{rl} is a fast converging series.

In view of (8), the tangential electric field continuity at $z = -b - d$ yields

$$\tilde{E}_y^{\mathrm{III}}(\zeta) = \sum_{l=-L_1}^{L_2}\sum_{m=1}^{\infty}[b_m^l \cos(\xi_m d) - c_m^l \sin(\xi_m d)]a_m a^2 e^{i\zeta lT}F_m(\zeta a). \quad (16)$$

Similarly, the tangential magnetic field continuity on the aperture of the slits $(rT - a < x < rT + a, z = -b - d: r = -L_1, \cdots, L_2)$ gives

$$-\frac{2k_z A_2}{\omega\mu_3}\beta_n^r + \frac{1}{2\pi\mu_3}\sum_{l=-L_1}^{L_2}\sum_{m=1}^{\infty} a_m a_n [b_m^l \cos(\xi_m d) - c_m^l \sin(\xi_m d)]a^2 I_{2mn}^{rl} = \frac{i}{\mu_2}a\xi_n[b_n^r \sin(\xi_n d) + c_n^r \cos(\xi_n d)] \quad (17)$$

where

$$\beta_n^r = a_n e^{ik_x rT}a^2 F_n(k_x a) \quad (18)$$

$$I_{2mn}^{rl} = \int_{-\infty}^{\infty} \kappa_3 a^2 F_m(\zeta a)F_n(-\zeta a)e^{i\zeta(l-r)T}\, d\zeta. \quad (19)$$

The evaluation of I_{2mn}^{rl} in the complex-ζ domain gives [6]

$$I_{2mn}^{rl} = \frac{2\pi\chi_m}{aa_m^2}\delta_{nm}\delta_{rl} - J_{2mn}^{rl} \quad (20)$$

where $\chi_m = \sqrt{k_3^2 - a_m^2}$ and J_{2mn}^{rl} is given by a rapidly convergent integral in the Appendix.

III. Evaluation of Scattered Fields

Equations (11) and (17) constitute a simultaneous system for c_m and b_m

$$\begin{bmatrix}\Psi_1 & \Psi_2\\ \Psi_3 & \Psi_4\end{bmatrix}\begin{bmatrix}B\\ C\end{bmatrix} = \begin{bmatrix}P\\ Q\end{bmatrix} \quad (21)$$

where B and C are column vectors of b_m and c_m, and the matrix elements are

$$\psi_{1,nm}^{rl} = \frac{a\eta_n \cot(\eta_n b)}{\mu_1}\delta_{mn}\delta_{rl} + \frac{1}{2\pi\mu_1}a_m a_n a^2 J_{1mn}^{rl} \quad (22)$$

$$\equiv \psi_1^{(0)}\delta_{mn}\delta_{rl} + \psi_1^{(1)} \quad (23)$$

$$\psi_{2,nm}^{rl} = \frac{1}{\mu_2}\xi_n a\delta_{nm}\delta_{rl} \quad (24)$$

$$\equiv \psi_2^{(0)}\delta_{mn}\delta_{rl} \quad (25)$$

$$\psi_{3,nm}^{rl} = \left[\frac{a\chi_n \cos(\xi_n d)}{\mu_3} - \frac{i}{\mu_2}a\xi_n \sin(\xi_n\, d)\right]\delta_{nm}\delta_{rl} - \frac{a_n a_m}{2\pi\mu_3}\cos(\xi_m\, d)a^2 J_{2mn}^{rl} \quad (26)$$

$$\equiv \psi_3^{(0)}\delta_{mn}\delta_{rl} + \psi_3^{(1)} \quad (27)$$

$$\psi_{4,nm}^{rl} = \left[-\frac{a\chi_n \sin(\xi_n\, d)}{\mu_3} - \frac{i}{\mu_2}a\xi_n \cos(\xi_n\, d)\right]\delta_{nm}\delta_{rl} + \frac{a_n a_m}{2\pi\mu_3}\sin(\xi_m\, d)a^2 J_{2mn}^{rl} \quad (28)$$

$$\equiv \psi_4^{(0)}\delta_{mn}\delta_{rl} + \psi_4^{(1)} \quad (29)$$

$$p_n^r = \frac{k_{zs}A_1}{\mu_1}\gamma_n^r \quad (30)$$

$$q_n^r = \frac{2k_z A_2}{\mu_3}\beta_n^r. \quad (31)$$

It is shown in [6] that J_{2mn}^{rl} is represented in asymptotic series of which sth term is on the order of $(k_3 a)^{0.5-s}$; hence, in high-frequency limit $(k_3 a \gg 1)$, we obtain an approximate closed-form

$$B \approx [\psi_2^{(0)}\psi_3^{(0)} - (\psi_1^{(0)} + \psi_1^{(1)})\psi_4^{(0)}]^{-1}(-\psi_4^{(0)}p_n^r + \psi_2^{(0)}q_n^r) \quad (32)$$

$$C \approx [\psi_2^{(0)}\psi_3^{(0)} - (\psi_1^{(0)} + \psi_1^{(1)})\psi_4^{(0)}]^{-1}(\psi_3^{(0)}p_n^r - \psi_1^{(0)}q_n^r). \quad (33)$$

Note that (32) and (33) ignore the branch-cut contribution $J_{2mn}^{rl}(= 0(1/\sqrt{k_3 a}))$, thereby significantly simplifying a computational amount. By use of the residue calculus, we evaluate

$$J_{1mn}^{rl} = -2\pi i\sum_{\gamma=1}^{\infty}\left.\frac{\kappa_1^2\{[(-1)^{m+n} + 1]e^{i\zeta|l-r|T} - (-1)^m e^{i\zeta|(l-r)T+2a|} - (-1)^n e^{i\zeta|(l-r)T-2a|}\}}{b\zeta(\zeta^2 - a_m^2)(\zeta^2 - a_n^2)a^2}\right|_{\zeta=\sqrt{k_1^2-(\gamma\pi/b)^2}} \quad (15)$$

the total scattered fields at $x = \pm\infty$

$$E_y^{\rm I}(\pm\infty, z) = \sum_v K_v^{\pm} \sin k_{zv}(z+b) e^{\pm ik_{xv}x} \quad (34)$$

where $0 < v < k_1 b/\pi, v$: integer, $k_{zv} = v\pi/b, k_{xv} = \sqrt{k_1^2 - k_{zv}^2}$

$$K_v^{\pm} = i \sum_{l=-L_1}^{L_2} \sum_{m=1}^{\infty} \frac{b_m^l a_m k_{zv} e^{\mp ik_{xv}lT} a^2 F_m(\mp k_{xv}a)}{k_{xv}b}. \quad (35)$$

When $A_1 = 1$ and $A_2 (= P_{i2}) = 0$, the time-averaged incident, reflected, transmitted and radiated [scattered into Region (III)] powers are, respectively

$$P_{i1} = \frac{k_{xs}b}{4\omega\mu_1} \quad (36)$$

$$P_r = \frac{1}{2}{\rm Re} \int_0^b E_y^I(-\infty, z) H_z^{\rm I*}(-\infty, z)\, dz = \frac{b}{4\omega\mu_1} \sum_v k_{xv} |K_v^-|^2 \quad (37)$$

$$P_t = \frac{1}{2}{\rm Re} \int_0^b [E_y^{i1}(\infty, z) + E_y^{\rm I}(\infty, z)][H_z^{i1}(\infty, z) + H_z^{\rm I}(\infty, z)]^*\, dz = \frac{b}{4\omega\mu_1}[k_{xs}|1 + K_s^+|^2 + \sum_{v\neq s} k_{xv}|K_v^+|^2] \quad (38)$$

$$P_s = \frac{1}{2}{\rm Re} \int_{-\infty}^{\infty} E_y^{\rm II}(x, -b-d) H_x^{\rm II*}(x, -b-d)\, dx = \sum_{l=-L1}^{L_2} \sum_{m=1}^{\infty} {\rm Re}\Big\{ \frac{-i\xi_m^* a}{2\omega\mu_2} \times [b_m^l \cos(\xi_m d) - c_m^l \sin(\xi_m d)] \cdot [b_m^l \sin(\xi_m d) + c_m^l \cos(\xi_m d)]^* \Big\} \quad (39)$$

where $0 < v < (k_1 b/\pi), v$: integer, and the symbols ${\rm Re}(\cdots)$ and $(\cdots)^*$ denote a real part and a complex conjugate of $(\cdots)$. The power conservation requires $P_r + P_t + P_s = P_{i1}$.

When $A_1 (= P_{i1}) = 0$ and $A_2 = 1$

$$P_{i2} = \frac{aNk_3}{\omega\mu_3} \quad (40)$$

$$P_r = \frac{1}{2}{\rm Re} \int_0^b E_y^{\rm I}(-\infty, z) H_z^{I*}(-\infty, z)\, dz = \frac{b}{4\omega\mu_1} \sum_v k_{xv} |K_v^-|^2 \quad (41)$$

$$P_t = \frac{1}{2}{\rm Re} \int_0^b E_y^{\rm I}(\infty, z) H_z^{I*}(\infty, z)\, dz = \frac{b}{4\omega\mu_1} \sum_v k_{xv} |K_v^+|^2. \quad (42)$$

The far-zone scattered field and power at distance $-x = r\sin\theta_s$ and $-(z + b + d) = r\cos\theta_s$ are

$$E_y^{\rm III}(r, \theta_s) = \sqrt{\frac{k_3}{2\pi r}} \cos\theta_s e^{i(k_3 r - \pi/4)} \tilde{E}_y^{\rm III}(\zeta)|_{\zeta = k_3 \sin\theta_s} \quad (43)$$

$$p_s(r, \theta_s) = \frac{1}{2}\, {\rm Re}[E_y^{\rm III}(r, \theta_s) H_\theta^{\rm III*}(r, \theta_s)]. \quad (44)$$

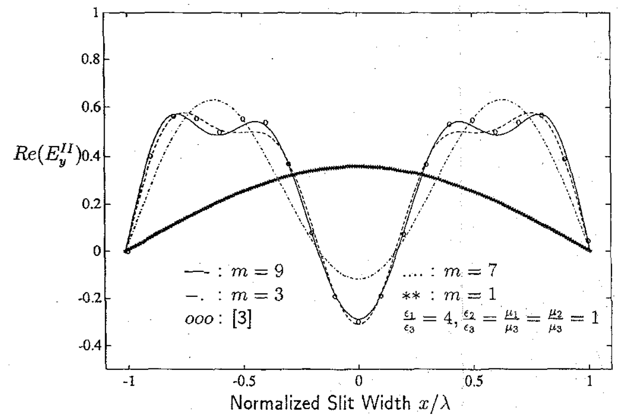

Fig. 2. Real part of $E_y^{\rm II}(x, -b-d)$ on the slit versus $x/\lambda (a = \lambda, b = 0.7\lambda, d = 0, A_1 = 0, A_2 = 1, N = 1)$.

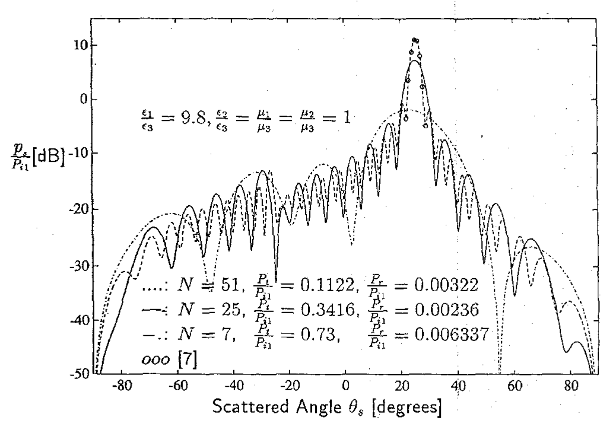

Fig. 3. Radiated power $p_s P_{i1}$ pattern when N is varied ($a = 0.165\lambda$, $b = 0.2\lambda$, $d = 0.035\lambda$, $T = 0.36\lambda$, $A_1 = 1, A_2 = 0$).

To check the accuracy of our computation, we compute $E_y^{\rm II}(x, -b-d)$ by varying m from one to nine and comparing our results to Fig. 3 of [3]. Fig. 2 shows that agreement between two results is excellent when $m = 9$ is used in our computation to achieve convergence. Fig. 3 shows the effects of N on the angular behavior of far-zone radiation from finite thin slits. As N increases from 7 to 51, the radiation pattern becomes sharper while retaining the maximum radiation at $\theta_s = 25°$. Note that our result with $N = 51$ agrees reasonably well with the theoretical prediction of infinite number of slits in [7]. We use $m = 2$ in the computation; hence, the size of the matrix (21) is 204×204. In Fig. 4 we investigate the accuracy of the high-frequency solution (32) and (33) when $a = 2.1\lambda$. The angular trend of p_s/P_{i1} between the high-frequency and exact solutions agrees very well except for more than a 3–4 dB level difference at $\theta_s > 20°$. The high-frequency solution requires no numerical integration of J_{2mn}^{rl}. This means that the high-frequency solution is very efficient for numerical computation yet accurate when $a > \lambda$. Fig. 5 shows the angle of the maximum radiation θ_{sm} versus the normalized aperture width $2a/\lambda$ for various T/λ. There exist abrupt changes in

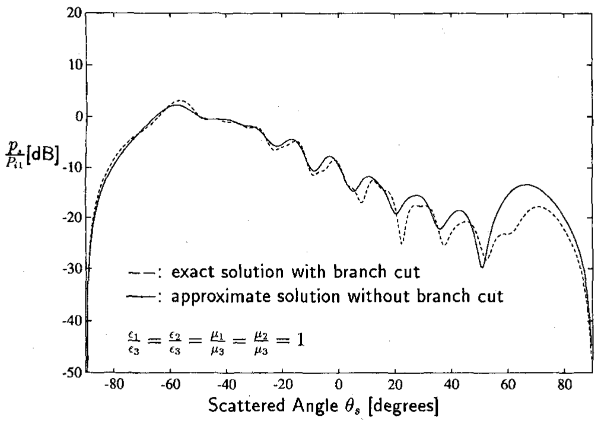

Fig. 4. Comparison of high-frequency limit pattern (p_s/P_{i1}) with exact one $(a = 2.1\lambda, b = 0.6\lambda, d = 0.1\lambda, T = 5\lambda, A_1 = 1, A_2 = 0, N = 2)$.

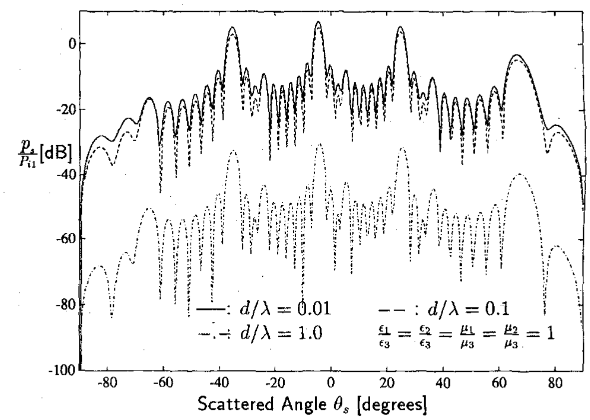

Fig. 6. Effects of d/λ on radiation pattern (p_s/P_{i1}) when $N = 10(a = 0.2\lambda,\ b = 0.6\lambda,\ T = 2\lambda,\ A_1 = 1, A_2 = 0)$.

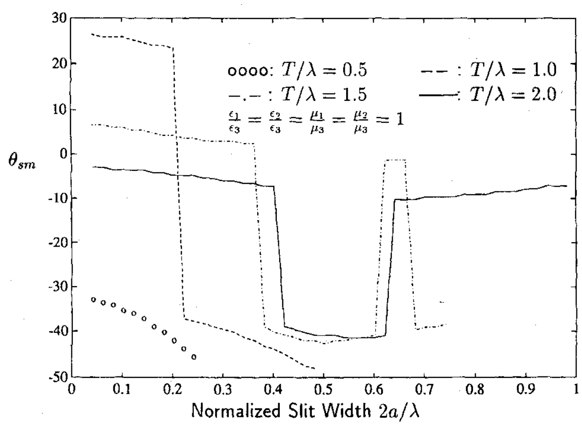

Fig. 5. Maximum radiation angle θ_{sm} when $2a$ and T are varied. $(b = 0.6\lambda, d = 0, A_1 = 1, A_2 = 0, N = 10)$.

θ_{sm} and θ_{sm} is limited to $-50° < \theta_{sm} < 30°$ for the choice of parameters considered here. Fig. 6 shows the effects of d/λ on the radiation pattern. As d/λ increases from 0.01 to 1, the level of p_s/P_{i1} decreases by more than 25 dB, whereas the angular shape of p_s/P_{i1} remains unchanged.

IV. Conclusion

The problem of TE-wave scattering and radiation from a finite thick slits in a parallel-plate is considered. The solution is obtained in simple series form which is very efficient for numerical computation. The computed results agree favorably with other existing solutions. The high-frequency-limit solution in analytic form, which requires no numerical integration, is shown to be valid for $a > \lambda$. The range of the maximum radiation from the slits is presented for various antenna geometry. The solution presented in the paper is useful for the design of the leaky wave antenna of slotted parallel-plate waveguide. It is straightforward to apply the presented approach to the problem of TM-wave scattering and radiation from finite thick slits in parallel-plate waveguide.

Appendix
Evaluation of Integral I^{rl}_{2mn}

The detailed evaluation of I^{rl}_{2mn} is given in [6]. The results are

1) When $l = r$ and $(m+n)$ is odd, $I^{rl}_{2mn} = 0$.
2) When $l = r$ and $(m+n)$ is even

$$I^{rl}_{2mn} = \frac{2\pi\chi_n}{a a_m^2}\delta_{mn}\delta_{lr} - J^{rl}_{2mn}$$
$$J^{rl}_{2mn} = R_1 + R_2$$

where

$$R_1 = \int_0^\infty \frac{-4i(-1)^n\sqrt{v(-2i+v)}e^{2ik_3a}e^{-2k_3av}}{(k_3a)^2[(1+iv)^2-\alpha^2][(1+iv)^2-\beta^2]}\,dv$$
$$R_2 = \int_0^\infty \frac{4i\sqrt{v(-2i+v)}}{(k_3a)^2[(1+iv)^2-\alpha^2][(1+iv)^2-\beta^2]}\,dv$$
$$\alpha = a_m/k_3, \qquad \beta = a_n/k_3.$$

3) When $l \neq r$

$$I^{rl}_{2mn} = \frac{2\pi\chi_n}{a a_m^2}\delta_{mn}\delta_{lr} - J^{rl}_{2mn}$$
$$J^{rl}_{2mn} = 2\{[(-1)^{m+n}+1]I_3(qT) - (-1)^m I_3(qT+2a) - (-1)^n I_3(qT-2a)\}$$

where

$$q = l - r$$
$$I_3(c) = \int_0^\infty \frac{i\sqrt{v(-2i+v)}e^{ik_3|c|}e^{-k_3|c|v}}{(k_3a)^2[(1+iv)^2-\alpha^2][(1+iv)^2-\beta^2]}\,dv.$$

References

[1] Y. K. Cho, "Analysis of a narrow slit in a parallel-plate transmission line: E-polarization case," *Electron. Lett.*, vol. 23, no. 21, pp. 1105–1106, Oct. 1987.
[2] H. A. Auda, "Quasistatic characteristics of a slotted parallel-plate waveguides," in *IEEE Proc.—Pt. H*, vol. 135, no. 4, pp. 256–262, Aug. 1988.

[3] C. W. Chuang, "Generalized admittance matrix for a slotted parallel-plate waveguide," *IEEE Trans. Antennas Propagat.*, vol. 36, no. 9, pp. 1227–1230, Sept. 1988.
[4] J. A. Encinar, "Mode-matching and point-matching techniques applied to the analysis of metal-strip-loaded dielectric antennas," *IEEE Trans. Antennas Propagat.*, vol. 38, no. 9, pp. 1405–1412, Sept. 1990.
[5] J. H. Lee, H. J. Eom, and K. Yoshitomi, "TE-mode scattering from finite rectangular grooves in parallel-plate waveguide," *Radio Sci.*, vol. 29, no. 5, pp. 1215–1218, Feb. 1994.
[6] T. J. Park, H. J. Eom, and K. Yoshitomi, "Analysis of TM scattering from finite rectangular grooves in a conducting plane," *J. Opt. Soc. Amer. A*, vol. 10, no. 5, pp. 905–911, May 1993.
[7] V. I. Kalinichev and Yu. V. Kuranov, "Diffraction of surface waves by an array of metallic rods and analysis of a leaky wave dielectric antenna," *Radiotekhnika i Elektronika*, no. 10, pp. 1902–1909, 1991.

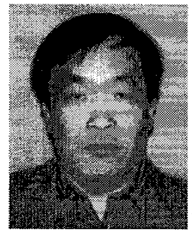

Hyo Joon Eom (S'78–M'82) received the B.S. degree in electronic engineering from Seoul National University, Korea, and the M.S. and Ph.D. degrees in electrical engineering from the University of Kansas, Lawrence, KS, in 1977 and 1982, respectively.

From 1981–1984, he was a Research Associate at the Remote Sensing Laboratory of the University of Kansas. From 1984–1989, he was with the faculty of the Department of Electrical Engineering and Computer Science, University of Illinois, Chicago, IL. In 1989, he joined the Department of Electrical Engineering, Korea Advanced Institute of Science and Technology where he is currently a Professor. His research interests are radar remote sensing and wave diffraction and scattering.

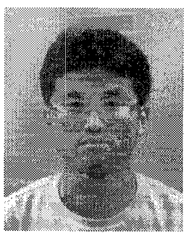

Jung H. Lee was born in Korea in 1968. He received the B.S. and M.S. degrees in electrical engineering from the Korea Advanced Institute of Science and Technology where he is now working toward the Ph.D. degree.

His area of interest is microwave measurement techniques and computational electromagnetics.

Jae W. Lee was born in Korea in 1970. He received the B.S. degree in electronic engineering from the Hanyang University, Seoul, Korea, in 1992, and the M.S. degree in electrical engineering from the Korea Advanced Institute of Science and Technology, in 1994. He is now working toward the Ph.D. degree in electrical engineering at the Korea Advanced Institute of Science and Technology at Taejon, Korea, with an emphasis in electromagnetics.